

*Supporting Information for*

**Interface Engineering of Ag-Ni<sub>3</sub>S<sub>2</sub> heterostructures toward Efficient Alkaline Hydrogen Evolution**

Caichi Liu,<sup># a</sup> Fangqing Wang,<sup># a</sup> Dongbo Jia<sup>a</sup>, Jingqian Zhang<sup>a</sup>, Jingyu Zhang<sup>a</sup>,  
Qiuyan Hao<sup>a</sup>, Jun Zhang<sup>a, c</sup>, Ying Li\*<sup>a</sup> and Hui Liu\*<sup>a, b</sup>

<sup>a</sup> School of Material Science and Engineering, Hebei University of Technology,  
Dingzigu Road 1, Tianjin 300130, P. R. China

<sup>b</sup> Department of Physics and Astronomy, University of California, Irvine, CA 92697,  
USA

<sup>c</sup> Hebei Key Laboratory of Boron Nitride Micro and Nano Materials, Guangrongdao  
Road 29, Tianjin 300130, P. R. China.

**Turnover frequency (TOF) calculation:** Turnover frequency is used to reflect the number of reactant molecule conversions per active site per unit time. Assuming that all Ni atoms participate in HER, according to the following formula:

$$\text{TOF} = \frac{j \times A}{2 \times n \times F}$$

Where j is the measured current density, A is the surface area of the electrocatalyst, F is the Faraday constant (96485.3 C mol<sup>-1</sup>), and n is the number of moles of Ni on the electrode.

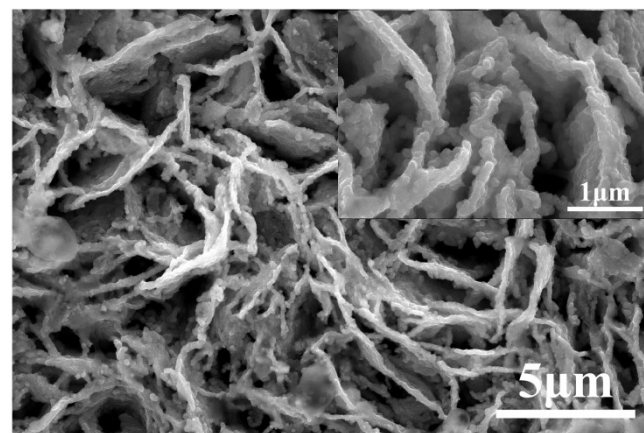


**Fig. S1.** SEM image of  $\text{Ni}_3\text{S}_2/\text{NF}$ .

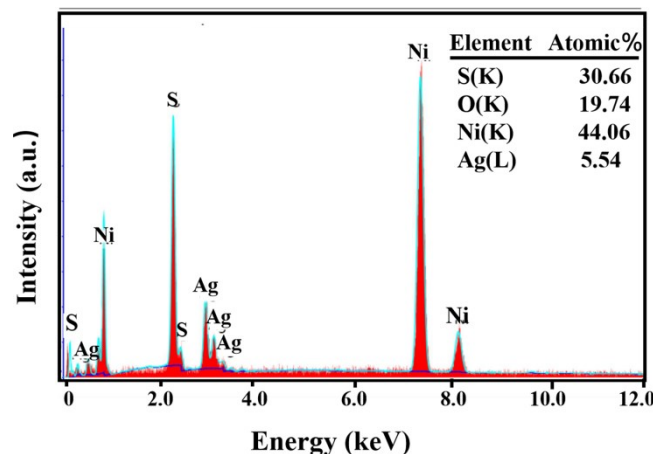


**Fig. S2.** EDS image of  $\text{Ag-Ni}_3\text{S}_2/\text{NF}$ -5min.

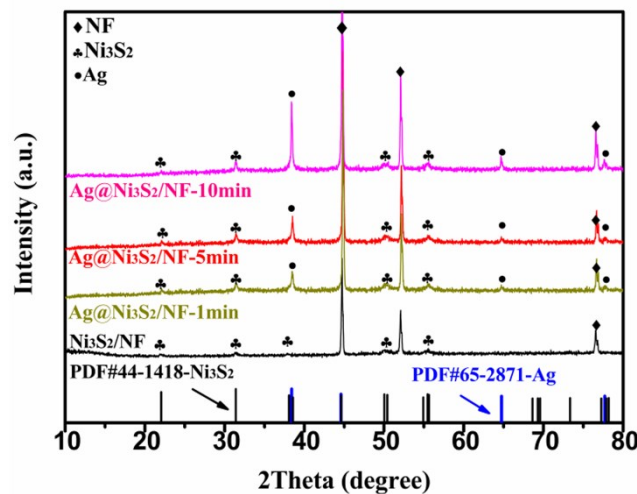


**Fig. S3.** XRD pattern of  $\text{Ag-Ni}_3\text{S}_2/\text{NF}$ -1min,  $\text{Ag-Ni}_3\text{S}_2/\text{NF}$ -5min,  $\text{Ag-Ni}_3\text{S}_2/\text{NF}$ -10min and  $\text{Ni}_3\text{S}_2/\text{NF}$ .

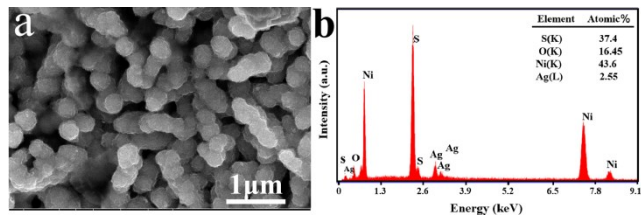


**Fig. S4.** (a) SEM image, (b) EDS spectrum of Ag-Ni<sub>3</sub>S<sub>2</sub>/NF-1min.

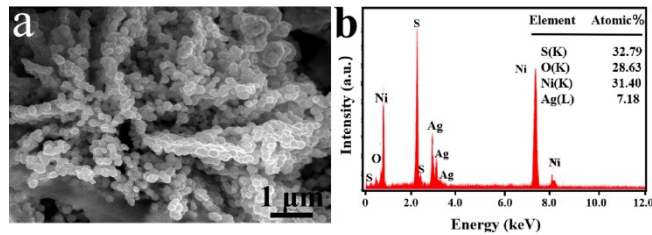


**Fig. S5.** (a) SEM image, (b) EDS spectrum of Ag-Ni<sub>3</sub>S<sub>2</sub>/NF-10min.

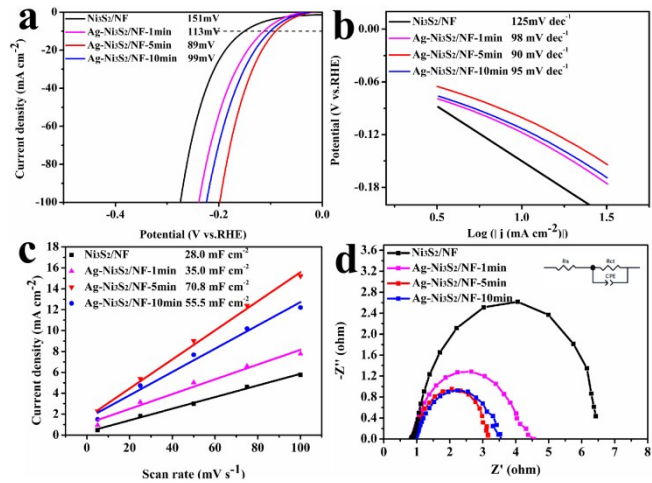


**Fig. S6.** (a) LSV curves, (b) Tafel slope, (c) Calculated electrochemical double-layer capacitances and (d) Nyquist plots of Ni<sub>3</sub>S<sub>2</sub>/NF and Ag-Ni<sub>3</sub>S<sub>2</sub>/NF with different Ag loading amount toward HER in 1M KOH.

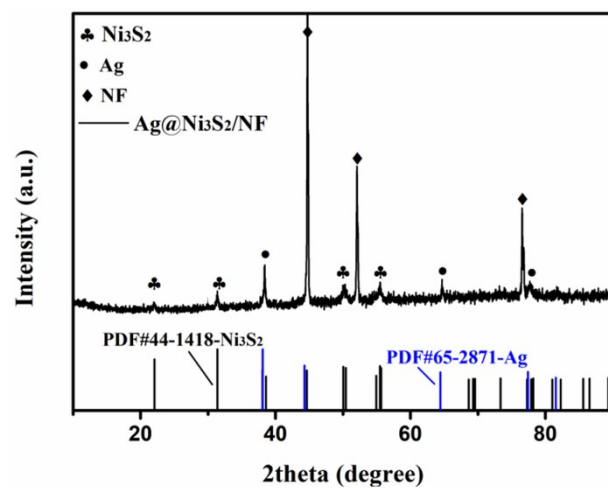


**Fig. S7.** XRD pattern of Ag-Ni<sub>3</sub>S<sub>2</sub>/NF after a stability test for 15 h.

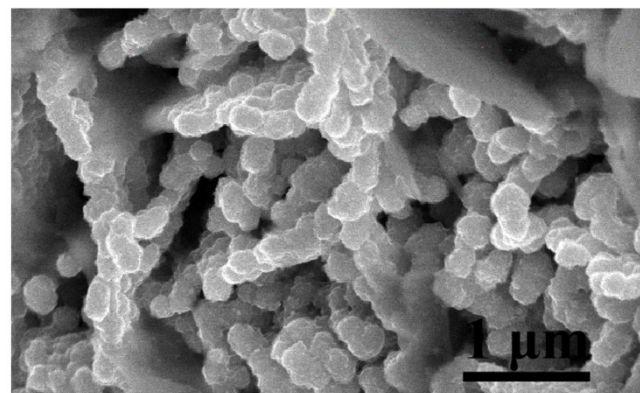


**Fig. S8.** SEM image of Ag-Ni<sub>3</sub>S<sub>2</sub>/NF after a stability test for 15 h.

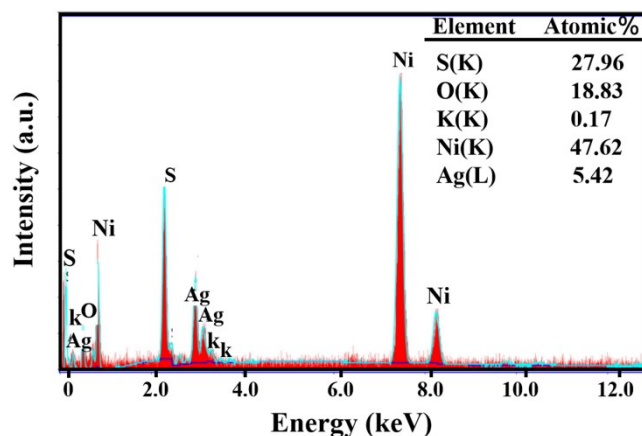


**Fig. S9.** EDS spectrum of Ag-Ni<sub>3</sub>S<sub>2</sub>/NF after a stability test for 15 h.

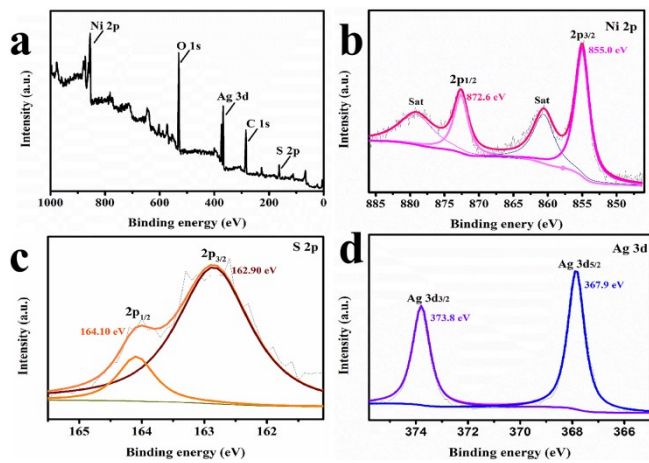


**Fig. S10.** (a) XPS survey, (b) Ni 2p, (c) S 2p, and (d)Ag 3d XPS spectra of Ag- $\text{Ni}_3\text{S}_2/\text{NF}$  after a stability test for 15 h.

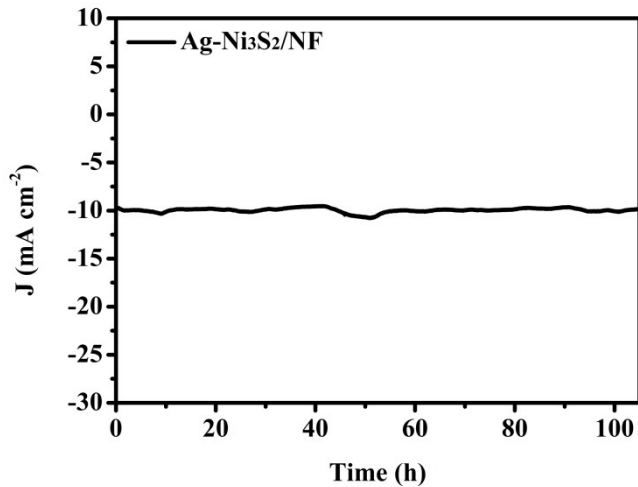


**Fig.S11.** long-term stability test curve of Ag- $\text{Ni}_3\text{S}_2/\text{NF}$  under an overpotential of -103 mV (vs RHE) for 105 h.

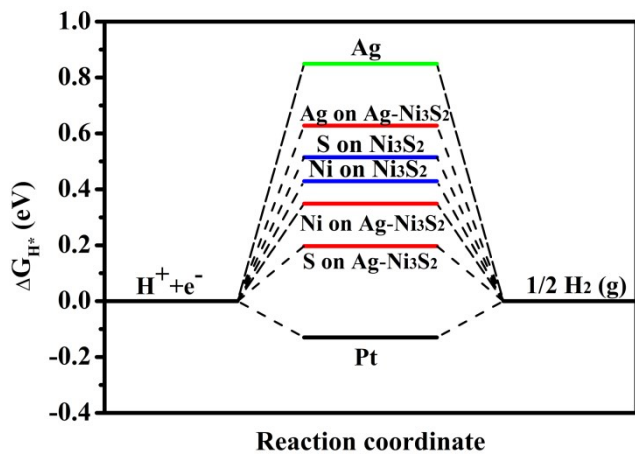


**Fig. S12.** Gibbs Free energy change of hydrogen on different sites of Ag-Ni<sub>3</sub>S<sub>2</sub> and Ni<sub>3</sub>S<sub>2</sub>.

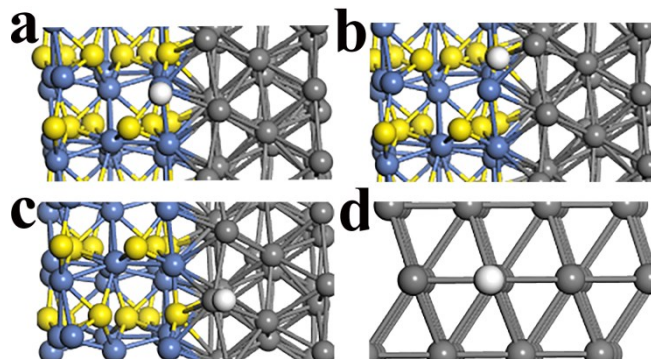


**Fig. S13.** DFT calculation models for  $\Delta G_{H^*}$  on (a) Ni site, (b) S site, (c) Ag site of Ag-Ni<sub>3</sub>S<sub>2</sub> and (d) Ag. (Hydrogen atom: white)

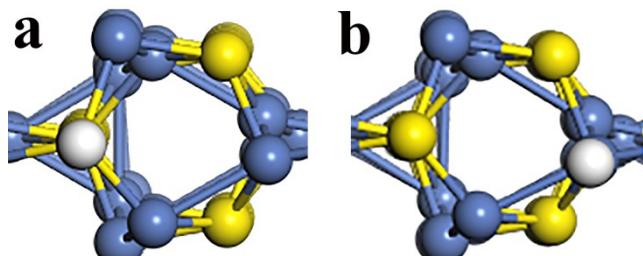


**Fig. S14.** DFT calculation models for  $\Delta G_{H^*}$  on (a) S site and (b) Ni site of Ni<sub>3</sub>S<sub>2</sub> (Hydrogen atom: white)

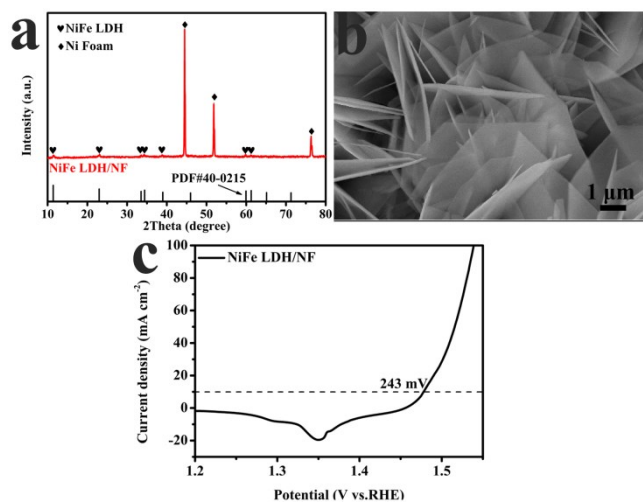


**Fig. S15.** (a) XRD pattern, (b) SEM image and (c) LSV curve of the NiFe LDH/NF in 1M KOH.

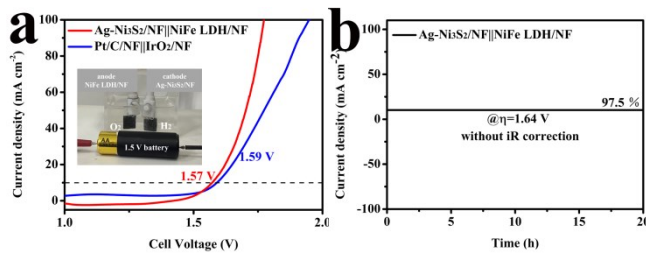


**Fig. S16.** (a) Overall water splitting performance LSV curves of Ag-Ni<sub>3</sub>S<sub>2</sub>/NF||NiFe LDH/NF, Pt/C/NF||IrO<sub>2</sub>/NF and Ni<sub>3</sub>S<sub>2</sub>/NF||Ni<sub>3</sub>S<sub>2</sub>/NF electrode pairs in 1 M KOH. (Inset: Image of a two-electrode water splitting unit driven by a battery with a rated voltage of 1.5 V) (b) Long-term stability test of Ag-Ni<sub>3</sub>S<sub>2</sub>/NF||NiFe LDH/NF for water splitting at 1.64 V.

**Table S1.** Loading amounts of Ag-Ni<sub>3</sub>S<sub>2</sub>/NF-1min, Ag-Ni<sub>3</sub>S<sub>2</sub>/NF-5min and Ag-Ni<sub>3</sub>S<sub>2</sub>/NF-10min.

Sample	Ag-Ni <sub>3</sub> S <sub>2</sub> /NF-1min	Ag-Ni <sub>3</sub> S <sub>2</sub> /NF-5min	Ag-Ni <sub>3</sub> S <sub>2</sub> /NF-10min
Loading amount (At %)	12.0%	26.5%	30.4%

**Table S2.** Comparison of the HER performance of Ag-Ni<sub>3</sub>S<sub>2</sub>/NF with other reported catalysts in 1 M KOH.

Catalysts	Overpotential at 10 mA cm <sup>-2</sup> (mV)	Tafel slope (mV dec <sup>-1</sup> )	References
Ag-Ni <sub>3</sub> S <sub>2</sub> /NF	89	90	This work
NF@Ni <sub>3</sub> S <sub>2</sub> @NCNT	~94	54	<sup>1</sup>
NF-Ni <sub>3</sub> S <sub>2</sub> /MnO <sub>2</sub>	102	69	<sup>2</sup>
NF/T(Ni <sub>3</sub> S <sub>2</sub> /MnS-O)	116	41	<sup>3</sup>
Ni <sub>3</sub> S <sub>2</sub> /MnS/NF	136	49	<sup>3</sup>
NiFe@Ni <sub>3</sub> S <sub>2</sub>	184	77	<sup>4</sup>
Cu NDs/Ni <sub>3</sub> S <sub>2</sub> NTs-CFs	128	76.2	<sup>5</sup>
CoMoNiS-NF	113	85	<sup>6</sup>
Co <sub>9</sub> S <sub>8</sub> -Ni <sub>3</sub> S <sub>2</sub> /NF	163	121	<sup>6</sup>
Ni <sub>x</sub> Co <sub>3-x</sub> S <sub>4</sub> /Ni <sub>3</sub> S <sub>2</sub> /NF	136	95	<sup>7</sup>
NiP	234	130	<sup>8</sup>
Ni <sub>3</sub> S <sub>2</sub> -300	177	75.5	<sup>9</sup>
Sn-Ni <sub>3</sub> S <sub>2</sub> /NF	137	51	<sup>10</sup>
P-(Ni,Fe) <sub>3</sub> S <sub>2</sub> /NF	98	88	<sup>11</sup>
Ni <sub>0.9</sub> Fe <sub>0.1</sub> PS <sub>3</sub> NS	72	73	<sup>12</sup>
Fe <sub>17.5%</sub> -Ni <sub>3</sub> S <sub>2</sub> /NF	47	95	<sup>13</sup>

**Table S3.** EIS and C<sub>dl</sub> results of Ni<sub>3</sub>S<sub>2</sub>/NF, Ag-Ni<sub>3</sub>S<sub>2</sub>/NF-1min, Ag-Ni<sub>3</sub>S<sub>2</sub>/NF-5min and Ag-Ni<sub>3</sub>S<sub>2</sub>/NF-10min.

---

Sample	Ni <sub>3</sub> S <sub>2</sub>	Ag-Ni <sub>3</sub> S <sub>2</sub> /NF-	Ag-Ni <sub>3</sub> S <sub>2</sub> /NF-	Ag-Ni <sub>3</sub> S <sub>2</sub> /NF-
		1min	5min	10min
R <sub>ct</sub> [Ω]	5.60	3.61	2.10	2.52
C <sub>dl</sub> [mF cm <sup>-2</sup> ]	28.00	35.00	70.80	55.50

---

## References

1. W. Zhou, J. Zhao, J. Guan, M. Wu and G. R. Li, *ACS omega*, 2019, **4**, 20244-20251.
2. Y. Xiong, L. Xu, C. Jin and Q. Sun, *Appl. Catal. B*, 2019, **254** 329-338.
3. Y. Zhang, J. Fu, H. Zhao, R. Jiang, F. Tian and R. Zhang, *Appl. Catal. B*, 2019, **257**, 117899.
4. X. Liang, Y. Li, H. Fan, S. Deng, X. Zhao, M. Chen, G. Pan, Q. Xiong and X. Xia, *Nanotechnology*, 2019, **30**, 484001.
5. J. X. Feng, J. Q. Wu, Y. X. Tong and G. R. Li, *J. Am. Chem. Soc.*, 2019, **141**, 13697-13697.
6. Y. Yang, H. Q. Yao, Z. H. Yu, S. M. Islam, H. Y. He, M. W. Yuan, Y. H. Yue, K. Xu, W. C. Hao, G. B. Sun, H. F. Li, S. L. Ma, P. Zapol and M. G. Kanatzidis, *J. Am. Chem. Soc.*, 2019, **141**, 10417-10430.
7. Y. Wu, Y. Liu, G.-D. Li, X. Zou, X. Lian, D. Wang, L. Sun, T. Asefa and X. Zou, *Nano Energy*, 2017, **35**, 161-170.
8. Z. Zhou, L. Wei, Y. Q. Wang, H. E. Karahan, Z. B. Chen, Y. J. Lei, X. C. Chen, S. L. Zhai, X. Z. Liao and Y. Chen, *J. Mater. Chem. A*, 2017, **5**, 20390-20397.

9. J. Dong, F.-Q. Zhang, Y. Yang, Y.-B. Zhang, H. He, X. Huang, X. Fan and X.-M. Zhang, *Appl Catal. B*, 2019, **243**, 693-702.
10. J. Yu, F. X. Ma, Y. Du, P. P. Wang, C. Y. Xu and L. Zhen, *Chemelectrochem*, 2017, **4**, 594-600.
11. C. Liu, D. Jia, Q. Hao, X. Zheng, Y. Li, C. Tang, H. Liu, J. Zhang and X. Zheng, *ACS Appl. Mater. Inter.*, 2019, **11**, 27667-27676.
12. B. Song, K. Li, Y. Yin, T. Wu, L. Dang, M. Caban-Acevedo, J. Han, T. Gao, X. Wang, Z. Zhang, J. R. Schmidt, P. Xu and S. Jin, *Acs Catalysis*, 2017, **7**, 8549-8557.
13. Zhang, G.; Feng, Y. S.; Lu, W. T.; He, D.; Wang, C. Y.; Li, Y. K.; Wang, X. Y.; Cao, F. F. *ACS Catal.* 2018, **8**, 5431-5441.